

## Supplementary Information for

### **Energy Level Modulation of Donor–Acceptor Alternating Random Conjugated Copolymers for Achieving High-Performance Polymer Solar Cells**

*Xi Liu,\* Wanyuan Deng, Junyi Wang, Ruiwen Zhang, Song Zhang, Luke Galuska, Shuting Pang, Xiaodan Gu, Xianfeng Qiao, Dongge Ma, Hongbin Wu, Chunhui Duan,\* Fei Huang,\* and Yong Cao*

#### **Experimental Section**

**General Details.** UV-vis spectra were recorded on a Shimadzu UV-3600 spectrophotometer. Cyclic voltammetry data were measured on a CHI600D electrochemical workstation by using Bu<sub>4</sub>NPF<sub>6</sub> (0.1 M) in acetonitrile as electrolyte and glassy-carbon, platinum, and saturated calomel electrode as the working, counter, and reference electrode, respectively. Potentials were referenced to the ferrocenium/ferrocene couple by using ferrocene as an internal standard. Molecular weights and molar-mass dispersity were determined with gel permeation chromatography at 150 °C on a PL-GPC 120 system using a PL-GEL 10 µm MIXED-B column and 1,2,4-trichlorobenzene as the eluent against polystyrene standards. All the polymer samples were dissolved in 1,2,4-trichlorobenzene at 150 °C overnight and the solutions were filtered through PTFE filters (0.2 µm) prior to injection. Thermogravimetric analyses (TGA) were measured using a NETZSCH TG 209 at a heating rate of 10 °C min<sup>-1</sup> with a nitrogen flow rate of 20 mL min<sup>-1</sup>. Differential scanning calorimetry (DSC) measurements were performed on a NETZSCH DSC200F3 Maia differential scanning calorimeter from 30 to 350 °C at a heating and cooling rate of 10 °C min<sup>-1</sup>.

**Fabrication and characterization of solar cells.** The BHJ OSCs with a conventional device structure of ITO/PEDOT:PSS/BHJ active layer/PFN-Br/Ag were fabricated. The indium tin oxide (ITO) glass substrates were cleaned by sequential sonication using acetone (15 min), detergent (15 min), deionized water (15 min, twice), and isopropanol (15 min), and then dried in oven at 70 °C before used. First, ITO substrates treated with oxygen plasma for 4 min, and PEDOT:PSS (CLEVIOS™ P VP AI 4083) was spin-coated on top of ITO substrates and annealed in air at 150 °C for 15 min to form ~40 nm layer. Subsequently, the active layer with an optimal thickness of ca. 100 nm was formed by spin-coating the mixed solution of the copolymers and [70]PCBM on top of the PEDOT:PSS layer. For polymer:ITIC devices, the active layer with an optimal thickness of ca. 105 nm was formed by spin-coating the mixed solution of polymer:ITIC (1:1, wt/wt) in chlorobenzene on top of the PEDOT:PSS layer, and followed with thermal annealing at 100 °C for 10 min. After spin-coating PFN-Br solution (0.5 mg/mL in methanol, 2000 rpm) of ~5 nm cathode interlayer, a 100 nm Ag layer were sequentially deposited by thermal evaporation through a shadow mask in a vacuum chamber at a pressure of  $4 \times 10^{-7}$  Torr. The active layer area of the device was defined to be 0.0516 cm<sup>2</sup>, which was further confined as 0.04 cm<sup>2</sup> by a non-refractive mask to improve the accuracy of measurements. The photovoltaic performance was measured under an AM 1.5G solar simulator (Taiwan, Enlitech SS-F5). The current density–voltage ( $J-V$ ) characteristics were recorded with a Keithley 2400 source meter. The light intensity was 100 mW cm<sup>-2</sup> as calibrated by a China general certification center (CGC) certified reference monocrystal silicon cell (Enlitech). The external quantum efficiency (EQE) spectra were performed on a commercial EQE measurement system (Taiwan, Enlitech, QE-R3011). The light intensity at each wavelength was calibrated

by a standard single-crystal Si photovoltaic cell. The photoelectric response of tail states was determined by a high-sensitive solar cell spectral response measurement system (QE-R, Enlitech Inc.), which was equipped with a SR570 amplifier for weak signal detection, and the incident light intensity was determined with calibrated silicon photodetector for wavelengths range from 300 nm to 1100 nm. The external quantum efficiency of electroluminescence was determined by measuring the emitted photons of forward biased photovoltaic devices in all directions through an integrated sphere by using a calibrated spectrometer (QE Pro, Ocean Optics).

**Fabrication and characterization of single-carrier devices.** Devices were fabricated to measure hole by using the space-charge-limited current (SCLC) method. The hole-only devices with a configuration of ITO/PEDOT:PSS (40 nm)/copolymer neat film or copolymer:[70]PCBM blend film/MoO<sub>x</sub> (10 nm)/Ag (100 nm). The data were analyzed according to the Mott–Gurney laws that includes a Poole–Frenkel-type dependence of mobility on the electric field, given by  $J = (9/8)\epsilon_r\epsilon_0\mu_0(V^2/d^3)\exp(0.89\gamma(V/d)^{1/2})$ , where  $\epsilon_0$  is the permittivity of free space,  $\epsilon_r$  is the dielectric constant of the polymer which is assumed to be around 3 for the conjugated polymers,  $\mu_0$  is the zero-field mobility,  $V$  is the voltage drop across the device,  $d$  is the film thickness of the active layer, and  $\gamma$  is a parameter that describes the strength of the field-dependence effect. The applied voltage is used without correcting for series resistance or built-in voltage. The hole and electron mobilities are extracted with the fit parameters at an electric field ( $E$ ) of  $1 \times 10^5$  V cm<sup>-1</sup> by the Murgatroyd equation  $\mu = \mu_0\exp(\gamma(E)^{1/2})$ .

**PL quenching experiments.** The PL quenching experiments were recorded by Shimadzu RF-6000 spectrometer @ different excitation wavelengths for the corresponding films.

**Transmission electron microscopy (TEM).** Transmission electron microscopy was performed on a Tecnai G2 Sphera transmission electron microscope (FEI) operated at 200 kV.

**Grazing incidence wide-angle X-ray scattering (GIWAXS).** The X-ray diffraction measurements were performed at the Stanford Synchrotron Radiation Light source (SSRL) on beamline 11-3 with an area detector (Rayonix mar CCD225). The X-ray beam with an energy of 12.735 keV and an incidence angle of  $0.12^\circ$  was used. The sample was kept in a helium chamber to avoid air scattering. Data reduction was performed using Igor software with Nika package.

**Synthesis of 2TBX-Br:** A solution of compound **1** (94 mg, 0.29 mmol) in tetrahydrofuran (10 mL) was cooled to 0 °C in dark. *N*-bromosuccinimide (136 mg, 0.77 mmol) was added by several part portions. The reaction mixture was warmed to room temperature, stirred overnight and concentrated in vacuum. The residue was purified by recrystallization from chloroform to get the product as an orange solid (110 mg, 80%). **<sup>1</sup>H NMR** (400 MHz, CDCl<sub>3</sub>, δ): 8.08 (d, 2H), 7.24 (d, *J* = 4 Hz, 2H). **<sup>13</sup>C NMR** (100 MHz, CDCl<sub>3</sub>, δ): 145.60, 145.39, 142.91, 142.33, 126.22, 122.66, 122.24. 14.1. **HRMS** (MALDI+) Calcd for C<sub>14</sub>H<sub>4</sub>Br<sub>2</sub>F<sub>2</sub>N<sub>2</sub>O<sub>2</sub>(M<sup>+</sup>): 478.12, Found: 476.63.

**Synthesis of Random Copolymers:** Tris(dibenzylideneacetone)-dipalladium(0) (2.47 mg, 0.0027 mmol) and tri(*o*-tolylphosphine) (6.57 mg, 0.0216 mmol) were added to a degassed solution of the BDT monomer (BDT-Sn) (0.09 mmol), and the dibrominated monomers (0.09 mmol in total) with the desired feeding ratio (2TBT-Br:BT-Br = 0.35:0.65 in molar ratio for P2TBT-BT, 2TBX-Br:BT-Br = 0.35:0.65 in molar ratio for P2TBX-BT, 2TBT-Br:BX-Br = 0.35:0.65 in molar ratio for P2TBT-BX, and 2TBX-Br:BX-Br = 0.35:0.65 in molar ratio for P2TBX-BX) in anhydrous *o*-xylene (1.6 mL) and anhydrous *N,N*-dimethylformamide (DMF) (0.2 mL). The mixture was stirred at 120 °C overnight, after which 2-(tributylstannyl)thiophene and 2-bromothiophene were sequentially added to the reaction mixture with 2 hour intervals. After another 2 hours, the reaction mixture was diluted with *ortho*-dichlorobenzene (*o*-DCB) and refluxed with ethylenediaminetetraacetic acid dipotassium salt dihydrate (EDTA) (100 mg) for 2 hours. Upon cooling to room temperature, the reaction mixture was precipitated in methanol and filtered through a Soxhlet thimble. The polymer was subjected to sequential Soxhlet extraction with acetone, hexane, and chloroform under argon protection. The chloroform fractions were concentrated under reduced pressure and precipitated in methanol to obtain the resulting copolymers.

P2TBT-BT: Yield (86%). GPC:  $M_n = 68$  kDa,  $D_M = 2.7$ .

P2TBX-BT: Yield (88%). GPC:  $M_n = 64$  kDa,  $D_M = 2.4$ .

P2TBT-BX: Yield (85%). GPC:  $M_n = 71$  kDa,  $D_M = 2.8$ .

P2TBX-BX: Yield (83%). GPC:  $M_n = 71$  kDa,  $D_M = 2.2$ .

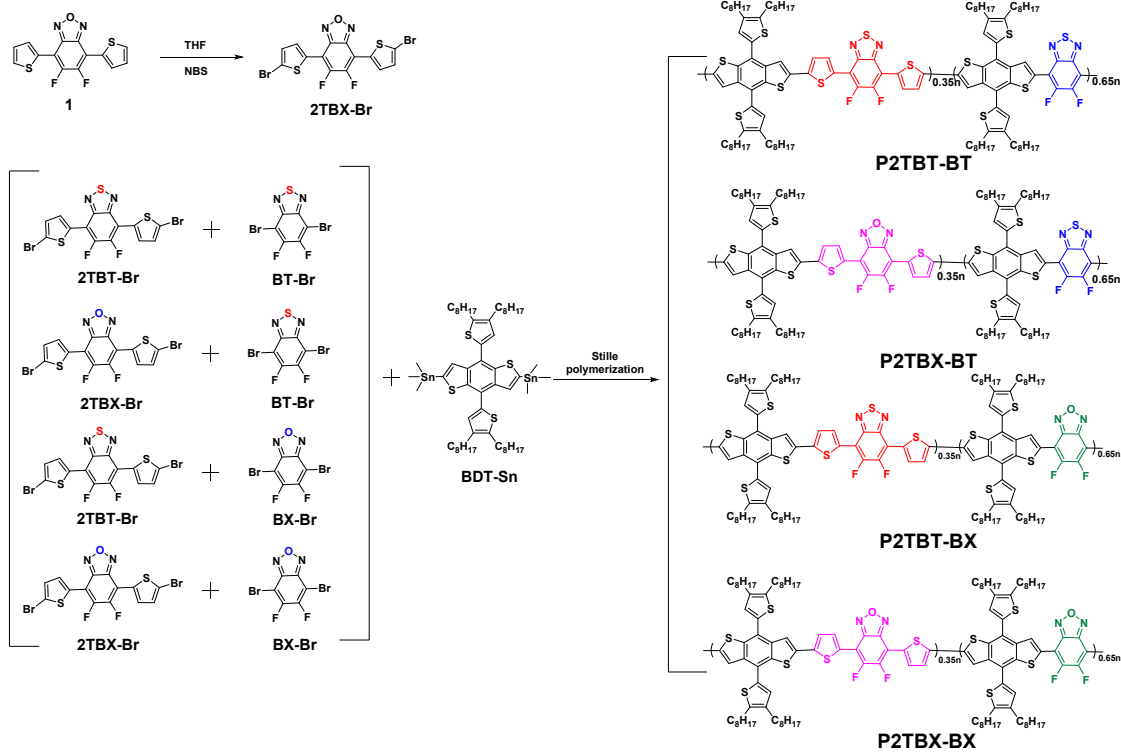


**Fig. S1.** Synthetic routes and chemical structures of the four random copolymers.

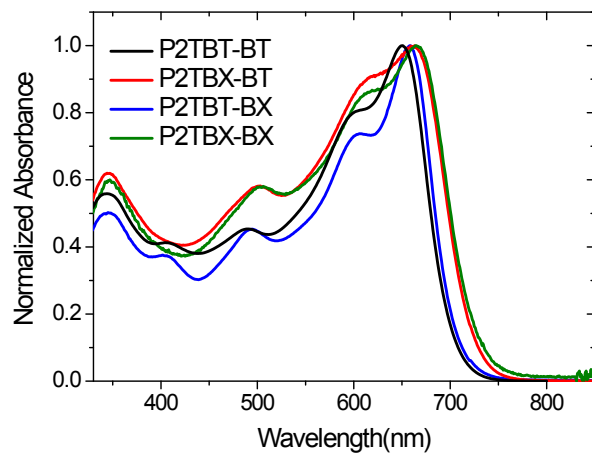


**Fig. S2.** Optical absorption spectra of the random copolymers in *o*-DCB solutions.

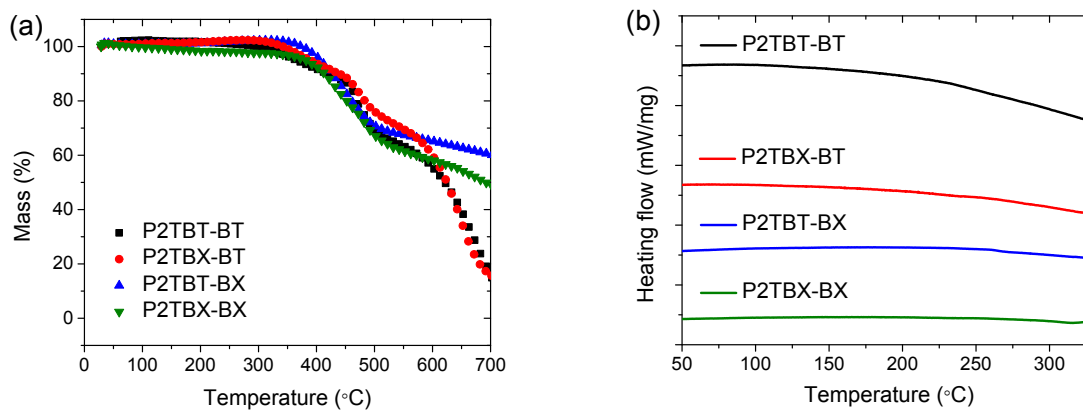


**Fig. S3.** TGA (a) and DSC (b) curves of the random copolymers.

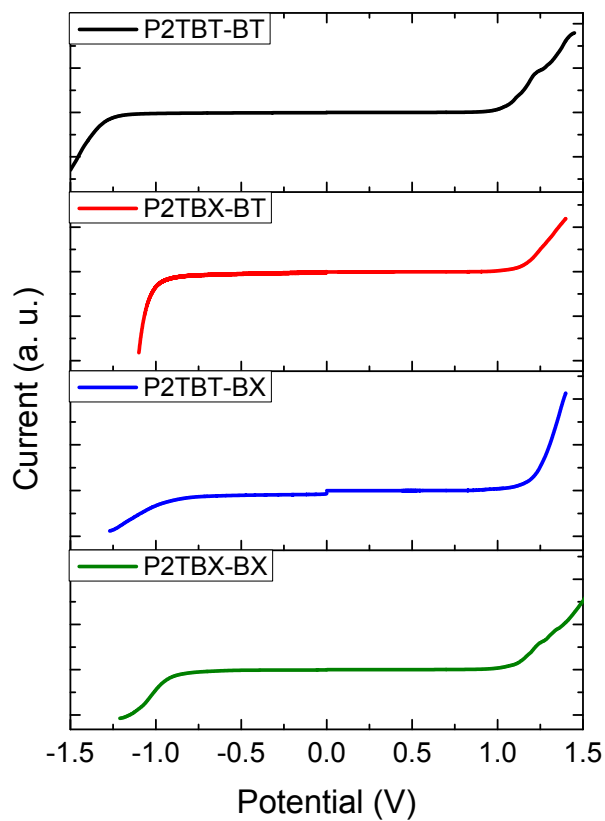


**Fig. S4.** Electrochemical CV curves of the random copolymers.

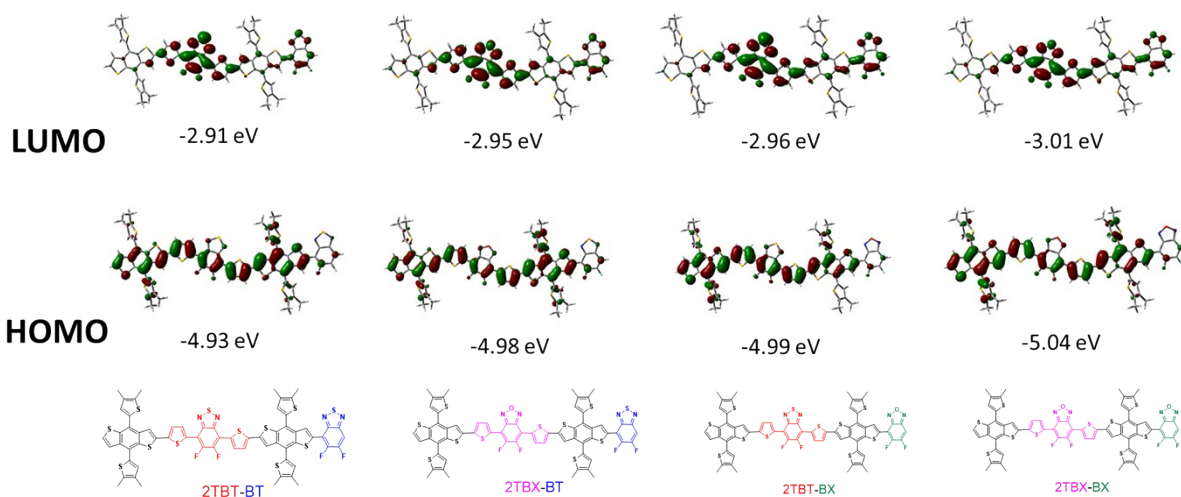


**Fig. S5.** DFT calculated results of the four specific structures.<sup>[1]</sup>

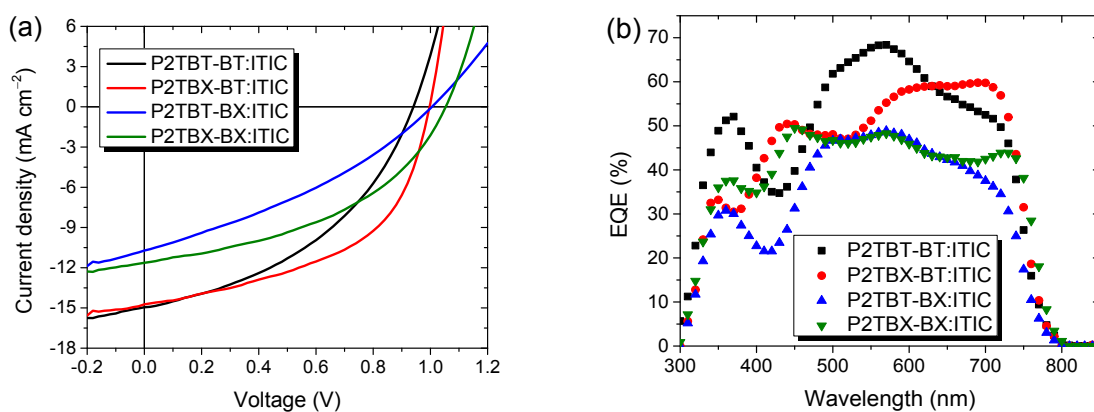


**Fig. S6.** (a) The  $J$ - $V$  curves of the devices under the illumination of AM1.5G ( $100 \text{ mW cm}^{-2}$ ), (b) EQE spectra of the PSCs based on the polymer:ITIC blends.

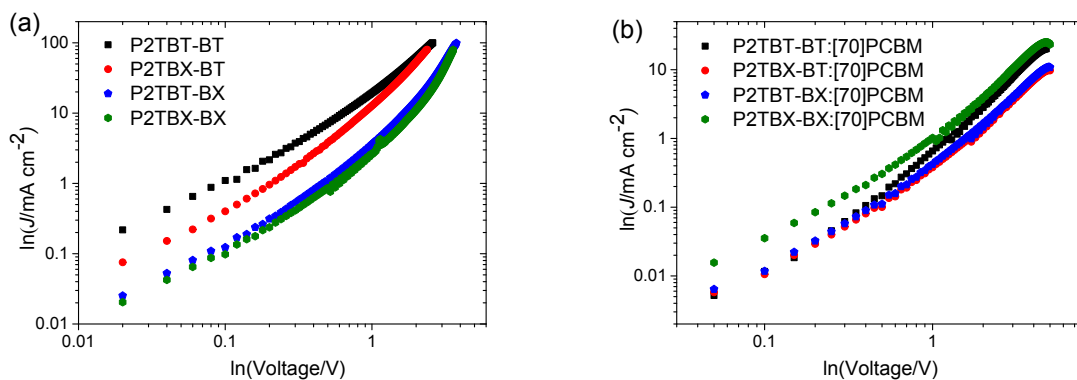


**Fig. S7.** The charge carriers mobilities characteristic in SCLC regions of hole-only devices for random copolymers neat films (a) and their blend films (b).

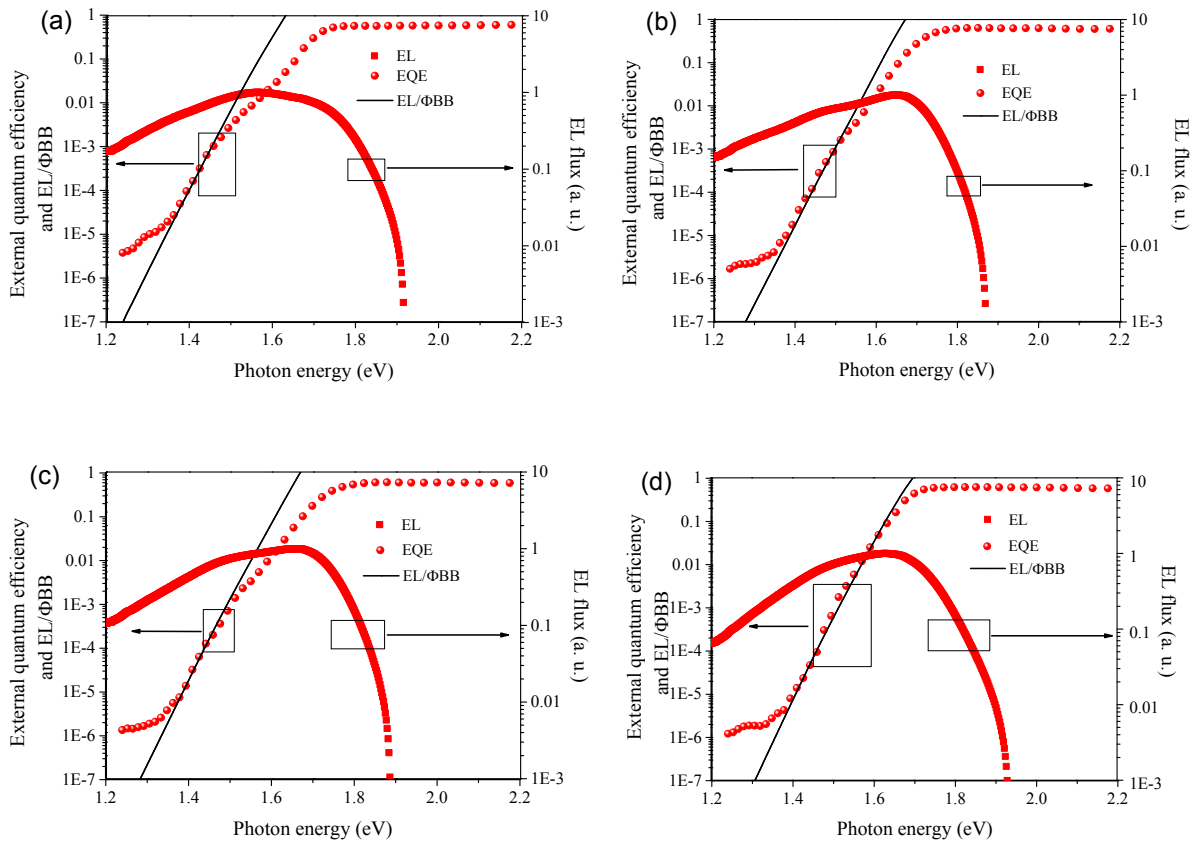


**Fig. S8.** External quantum efficiency, electroluminescence (EL), the black-body emission ( $\Phi_{BB}$ ), and EL flux for the devices based on P2TBT-BT:[70]PCBM (a), P2TBX-BT:[70]PCBM (b), P2TBT-BX:[70]PCBM (c), and P2TBX-BX:[70]PCBM (d).

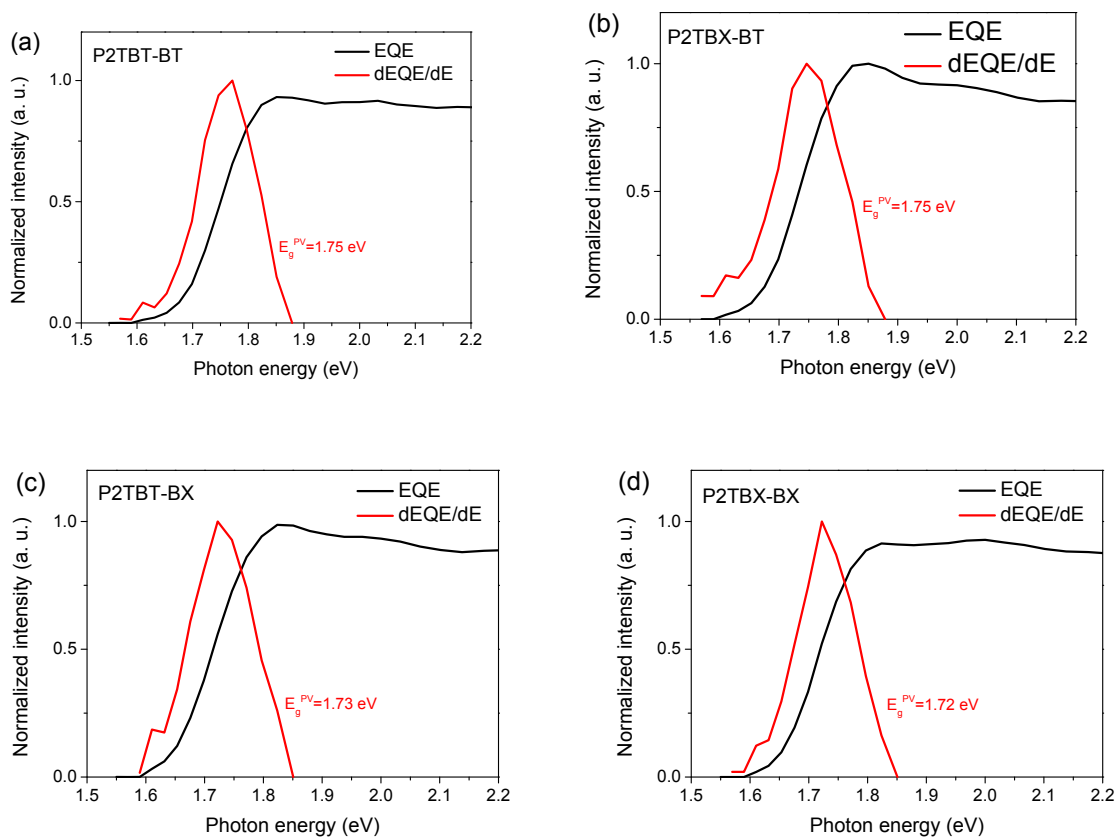


**Fig. S9.** Optical gap of photovoltaic devices for (a) P2TBT-BT, (b) P2TBX-BT, (c) P2TBT-BX and (d) P2TBX-BX, determined from the derivatives of external quantum efficiency curves<sup>[2]</sup>, denoted as  $E_g^{PV}$ .

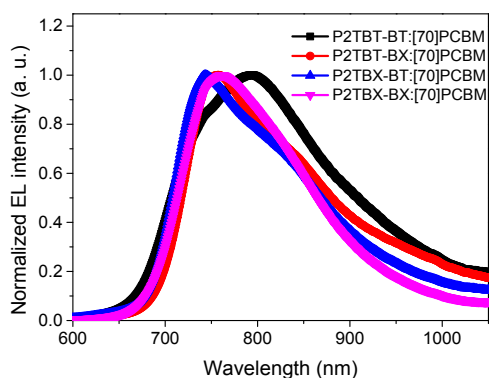


**Fig. S10.** EL spectra of the random copolymers based photovoltaic devices.

**Table S1.** The detailed photovoltaic properties of the PSCs based on the polymer:[70]PCBM blend under AM1.5G illumination at 100 mW cm<sup>-2</sup>.<sup>a)</sup>

Active layer	D/A ratio	Sol. Add.	Annealing	$V_{oc}$ [V]	$J_{sc}$ [mA cm <sup>-2</sup> ]	FF	PCE [%]	Thickness [nm]
P2TBX-BT:[70]PCBM	1:1	CB	–	0.90	13.0	0.64	7.5	101
			60 °C 5 min	0.90	13.0	0.63	7.4	99
	–		0.88	12.5	0.72	7.9	103	
	60 °C 5 min		0.87	11.9	0.67	7.0	105	
	1:3		–	0.91	12.3	0.60	6.8	104
P2TBX-BT:[70]PCBM	1:2	CB/ 3% CN	–	0.93	11.9	0.51	5.6	100
		CB/ 3% DPE	–	0.94	10.2	0.48	4.6	105
		CB/ 3% CBA	–	0.93	11.0	0.52	5.4	102
		CB/ 0.5% DIO	–	0.91	11.8	0.61	6.5	106
		CB/ 2% DIO	–	0.91	11.1	0.57	5.8	105
		CB/ 3% DIO	–	0.91	11.9	0.64	7.0	105
		CB/ 4% DIO	–	0.90	11.8	0.62	6.6	105
P2TBT-BT:[70]PCBM	1:2	CB	–	0.88	13.8	0.73	8.8	105
P2TBX-BT:[70]PCBM	1:2	CB	–	0.88	12.5	0.72	7.9	103
P2TBT-BX:[70]PCBM	1:2	CB	–	0.91	12.9	0.60	7.0	104
P2TBX-BX:[70]PCBM	1:2	CB	–	0.93	11.7	0.61	6.7	100

<sup>a)</sup>The detailed photovoltaic properties of the PSCs based on P2TBT-BT:[70]PCBM had exhibited in our previous work.<sup>[2]</sup>

**Table S2.** The photovoltaic properties of the PSCs based on the polymer:ITIC blend under AM1.5G illumination at 100 mW cm<sup>-2</sup>.

Active layer	$V_{oc}$ [V]	$J_{sc}$ [mA cm <sup>-2</sup> ]	FF	PCE [%]	EQE <sub>max</sub>
P2TBT-BT:ITIC	0.94	14.9	0.43	6.1	67%
P2TBX-BT:ITIC	1.00	14.7	0.51	7.5	56%
P2TBT-BX:ITIC	1.01	10.5	0.35	3.7	46%
P2TBX-BX:ITIC	1.06	11.5	0.42	5.2	46%

**Table S3.** Hole and electron mobilities obtained by SCLC method.

Test film	$\mu_h$ [cm <sup>2</sup> V <sup>-1</sup> s <sup>-1</sup> ]
P2TBT-BT	$3.4 \times 10^{-3}$
P2TBX-BT	$2.2 \times 10^{-3}$
P2TBT-BX	$1.3 \times 10^{-3}$
P2TBX-BX	$1.1 \times 10^{-3}$
P2TBT-BT:[70]PCBM	$1.6 \times 10^{-4}$
P2TBX-BT:[70]PCBM	$1.0 \times 10^{-4}$
P2TBT-BX:[70]PCBM	$1.1 \times 10^{-4}$
P2TBX-BX:[70]PCBM	$2.9 \times 10^{-4}$

**Table S4.** Lattice parameters of the four copolymers in neat films and in copolymer:[70]PCBM blend films.

Copolymers	Lamellar distance [Å]	$\pi$ - $\pi$ distance [Å]
P2TBT-BT	23.6	3.66
P2TBT-BT:[70]PCBM	22.3	3.51
P2TBX-BT	23.3	3.66
P2TBX-BT:[70]PCBM	22.3	3.62
P2TBT-BX	23.6	3.67
P2TBT-BX:[70]PCBM	22.2	3.61
P2TBX-BX	23.4	3.64
P2TBX-BX:[70]PCBM	22.3	3.54

## References

[1] M. J. Frisch, G. W. Trucks, H. B. Schlegel, G. E. Scuseria, M. A. Robb, J. R. Cheeseman, G. Scalmani, V. Barone, B. Mennucci, G. A. Petersson, H. Nakatsuji, M. Caricato, X. Li, H. P. Hratchian, A. F. Izmaylov, J. Bloino, G. Zheng, J. L. Sonnenberg, M. Hada, M. Ehara, K. Toyota, R. Fukuda, J. Hasegawa, M. Ishida, T. Nakajima, Y. Honda, O. Kitao, H. Nakai, T. Vreven, J. A. Montgomery Jr, J. E. Peralta, F. Ogliaro, M. Bearpark, J. J. Heyd, E. Brothers, K. N. Kudin, V. N. Staroverov, R. Kobayashi, J. Normand, K. Raghavachari, A. Rendell, J. C. Burant, S. S. Iyengar, J. Tomasi, M. Cossi, N. Rega, J. M. Millam, M. Klene, J. E. Knox, J. B. Cross, V. Bakken, C. Adamo, J. Jaramillo, R. Gomperts, R. E. Stratmann, O. Yazyev, A. J. Austin, R. Cammi, C. Pomelli, J. W. Ochterski, R. L. Martin, K. Morokuma, V. G. Zakrzewski, G. A. Voth, P. Salvador, J. J. Dannenberg, S. Dapprich, A. D. Daniels, O. Farkas, J. B. Foresman, J. V. Ortiz, J. Cioslowski and D. J. Fox, Gaussian 09, Revision A.02, Gaussian, Inc.,

Wallingford CT, 2009.

[2] Y. Wang, D. Qian, Y. Cui, H. Zhang, J. Hou, K. Vandewal, T. Kirchartz and F. Gao, *Adv. Energy Mater.*, 2018, **8**, 1801352.

[3] C. Duan, K. Gao, J. J. van Franeker, F. Liu, M. M. Wienk and R. A. J. Janssen, *J. Am. Chem. Soc.*, 2016, **138**, 10782.